Available online at www.sciencedirect.com
SCIENCE DIRECT®
Journal of Power Sources 123 (2003) 137–150
JOURNAL OF POWER SOURCES
www.elsevier.com/locate/jpowsour

Improvement in methanol oxidation in a centrifugal field

H. Cheng, K. Scott*

School of Chemical Engineering & Advanced Materials, University of Newcastle upon Tyne, Newcastle upon Tyne NE1 7RU, UK

Received 29 October 2002; received in revised form 24 February 2003; accepted 24 March 2003

Abstract

Oxidation of methanol at a Pt–Ru/Ti mini-mesh anode has been investigated. The oxidation is efficient giving low anode potential, e.g. 520 mV versus RHE at a current density of 200 mA cm^{-2}. The potentials were lower than that obtained at catalysed carbon cloth anode and at catalysed Teflon-bonded gas diffusion anode, under similar conditions. An outstanding performance was demonstrated by subjecting the electrolytic cell, including the electrolytes, to centrifugal force to enhance mass transfer and to accelerate gas bubble disengagement from the electrode surfaces, the electrolytes and the membrane. The acceleration field caused a significant reduction in the anode potential (up to 500 mV at 300 mA cm^{-2}), compared with a static cell, and increased current density greatly by up to 250 mA cm^{-2} at 500 mV versus RHE, at a relative acceleration rate of 190 and at 80 °C. Increasing the methanol concentration and the electrolyte temperature increased the rate of methanol oxidation. An increase in the concentration of the electrolyte led to a reduction in the cell resistance. These improvements in anode potential were improved further in a centrifugal field, compared to a gravitational field.

Keywords: Methanol oxidation; Process intensification; Centrifugal fields; Pt–Ru anode

1. Introduction

The direct methanol fuel cell (DMFC) has undergone much of investigations due to its potential world markets for various stationary and mobile applications [1–8]. In principle, methanol would be an ideal fuel owing to its low cost, good availability, liquid form and high volumetric energy density. The methanol oxidation reaction can be expressed as:

$$CH_3OH + H_2O = CO_2 + 6H^+ + 6e^- \quad \text{(acidic media)} \quad (1)$$

$$CH_3OH + 8OH^- = {CO_3}^{2-} + 6H_2O + 6e^- \quad \text{(alkaline media)} \quad (2)$$

The efficiency of the methanol oxidation, which determines the power level of a DMFC, is greatly depended on mass transfer rates, conduction of electrons in the electrode and charge transfer rates across the interface [9]. Mass transfer limitations were often observed in conventional methanol fuel cells. Moreover, the products of methanol oxidation, e.g. CO_2 bubbles, adhere to the anode surface and restrict access of methanol to the anode surface. This diminished the contribution of the catalysts and increased anode polarisation. These bubbles can also adhere to the membrane and are distributed in the electrolyte and therefore can increase the cell resistance.

An option to reduce the problems of gas bubbles is to design and operate a compact rotary electrochemical cell. When a centrifugal field is applied to such a cell, i.e. a multiphase system, according to theory, the light phase, e.g. gas, will flow inward, whereas the centrifugal effect will tend to sweep the denser fluid outward. This gives a rapid and efficient removal of the electrolytic gas product from the electrodes, the electrolytes and the membranes, resulting in considerable reduction in the resistance of the cell, with possible improvement in the cell efficiency. Since the energy in a centrifugal field is deployed within the liquid boundary layer, its impact on mass transfer process should be more effective than an equal amount discharged throughout the electrolyte, as with a pumped cell, for example. This has been observed in an investigation of the effect of a centrifugal field on the operation of a chlorine evolution cell [10].

Based on the above considerations, this work was undertaken to investigate methanol oxidation in a centrifugal field, i.e. the electrochemical cells is rotated in a laboratory centrifuge, in order to provide the basis for a more realistic and more efficient fuel cell design. It should be noted in this context that the energy needed to rotate the electrochemical

* Corresponding author. Tel.: +44-191-2228771; fax: +44-191-2611182.
E-mail address: k.scott@ncl.ac.uk (K. Scott).

0378-7753/$ – see front matter © 2003 Elsevier Science B.V. All rights reserved.
doi:10.1016/S0378-7753(03)00526-3

cell and overcome windage, friction, etc. will be quite small compared to that is capable of being saved [11].

2. Experimental

2.1. Centrifugal rig

Experiments were carried out in a centrifugal rig (Fig. 1), with a two-compartment membrane cell of 50 ml capacity (Fig. 2), operating under ambient pressure.

As shown in Fig. 1(a), the membrane cell (detailed later) was housed within the centrifuge pool. The electrochemical process intensification was realised in an acceleration field generated in a MSE Super Minor Centrifuge (UK) and monitoring by a computer-controlled potentiostat. To achieve higher temperature cell operation, hot compressed air was continuously introduced into the centrifuge pool using copper tubing. A thermocouple junction was attached to the air outlet tube to determine the temperature of the outlet air. Before starting experiments at elevated temperature, a preheating period of 30 min was required to reach a desired constant temperature.

Fig. 1(b) shows a plan view of the centrifuge system. The cell and its identical counter part (weight) were connected to the axis by the aid of stainless rotating rods, inserted into the cell and the counter part, and the fixed caps and the screws, fitted on the centrifuge axis. The cell, when operated stationary, was positioned vertically. When the cell was rotated it was in a horizontal position.

The distinctive feature of the electrolytic cell in this work is that both electrodes and electrolyte rotate at the same speed. There is no slip and negligible power dissipation and thus a low cost in operation. This is in marked contrast to other cells, for example, spinning disc or pump cells, in which there is a large electrolyte–electrode speed difference and a correspondingly high power loss.

Fig. 2(a) and (b) shows the side view and cross-sectional view of the rotary cell. The cell consisted of polyethylene blocks, each with internal volumes of 50 ml. The electrode was held between two electrically conducting meshes (usually made up of expanded Pt/Ti metal) in electrolyte "channels". The channels supply reactants to the respective sides of the electrode. Working and counter electrode chambers were fixed inside the cell blocks and separated by a membrane. The electrodes, membrane and the blocks were sealed by silicon rubber gaskets. The cell was held together between two blocks using a set of retaining bolts positioned around the periphery of the cell. Fig. 2(c) details the cross-sectional views of the working and counter chambers. The other details of the rig and cells are described elsewhere [12].

The Pt–Ru/Ti mini-mesh anode and the Pt/Ti mini-mesh cathode, made in this laboratory, were used. The "electrode area" used to calculate the current density was based on that projected onto the membrane. The reference electrode was made of Nafion® 117 membrane (DuPont), which connected to the conductive wire through a silicon gel block. There was a fixed distance (0.5 cm) between the reference electrode and the working electrode. The feasibility of the Nafion membrane reference electrode was evaluated under various experimental conditions and reported elsewhere [12]. The direct measurement of electrochemical parameters in centrifugal fields was achieved by using this reference electrode. All measurements were repeated with fresh electrolyte solutions, at least twice, under the same conditions to ensure reproducibility.

2.2. Preparation of catalysed electrodes

Catalysed Ti mini-mesh, as a novel technical electrode, is not commercially available. Published techniques [13–17] were modified and used to prepare catalysed electrodes by chemical and electrochemical deposition [12]. An impregnation method was employed to prepare Ti mini-mesh supported electrodes. The Ti mini-mesh surface was first abraded with emery paper and rinsed thoroughly with water. After drying, the Ti mesh was rinsed in acetone. Following etching with 20% HCl solution at 90 °C for 1 min, a catalyst slurry, e.g. $H_2PtCl_6 + H_2O$, was painted onto the substrates. The resulting paint was applied as a thin layer followed by thermal decomposition in air within a cubic furnace at 350–500 °C for 15–60 min. The process was repeated about 10 times to build up the desired coating thickness [12].

For electrochemical deposition, the Ti mini-mesh were pre-treated using the same method as that used in the chemical deposition prior to mounting into the deposition cell. The cell was then filled with N_2-saturated chloroplatinic acid and/or ruthenium chloride solution of known concentration and stirred mechanically. The catalyst was electrodeposited onto the substrate by controlling potential, which was chosen according to the linear sweep voltammograms. The amount of charge required to deposit the catalyst was monitored through a computer-controlled potentiostat. For co-electrodeposition of bimetallic deposits, e.g. Pt–Ru, a dual deposition strategy was used, i.e. depositing Ru followed by depositing Pt or vice verse. Following deposition, electrodes were extensively washed with boiling Millipore conductivity water until free from any chloride content. Both chemical and electrochemical depositions were carried out with a number of electrodes to check reproducibility. The platinum deposits obtained by the above procedure were bright and the ruthenium deposit tended to be dark grey in colour. The deposits appeared uniform to the eye and adhered well to the Ti mini-mesh, requiring forceful scratching to remove them [12].

The morphology and microstructure of the above catalysed electrodes was assessed by scanning electron microscopy (SEM) and scanning electron microprobe with an energy-dispersive X-ray (EDX) system. The measurements were carried out using a JEOL JSM-5300LV scanning electron microscope at an acceleration voltage of 25 kV. The

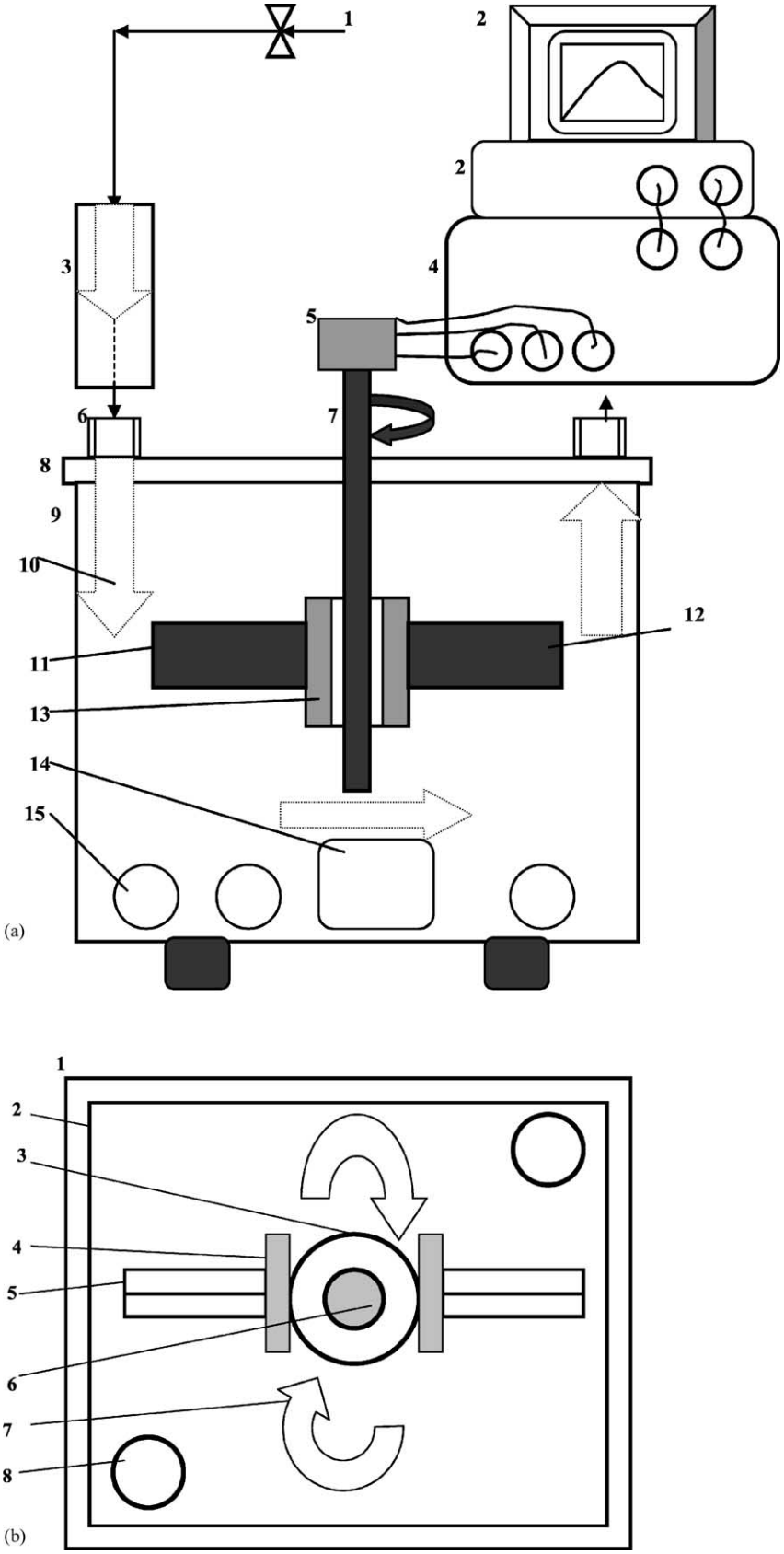

Fig. 1. Experimental equipment. (a) Side view of the centrifugal rig: (1) compressed air; (2) computer; (3) air heater; (4) potentiostat; (5) slip ring; (6) inlet or outlet of hot air; (7) axis; (8) cover of the centrifuge; (9) centrifuge; (10) hot air; (11) rotary cell; (12) counter part of the cell; (13) stainless steel rods and fixed caps and screws; (14) revolution meter; (15) control knobs. (b) Top plan view of the centrifuge assembly: (1) cover of the centrifuge; (2) centrifuge; (3) slip ring; (4) stainless steel rods and fixed caps and screws; (5) rotary membrane cell or the counter part of the cell; (6) axis; (7) rotation direction; (8) inlet or outlet of hot air.

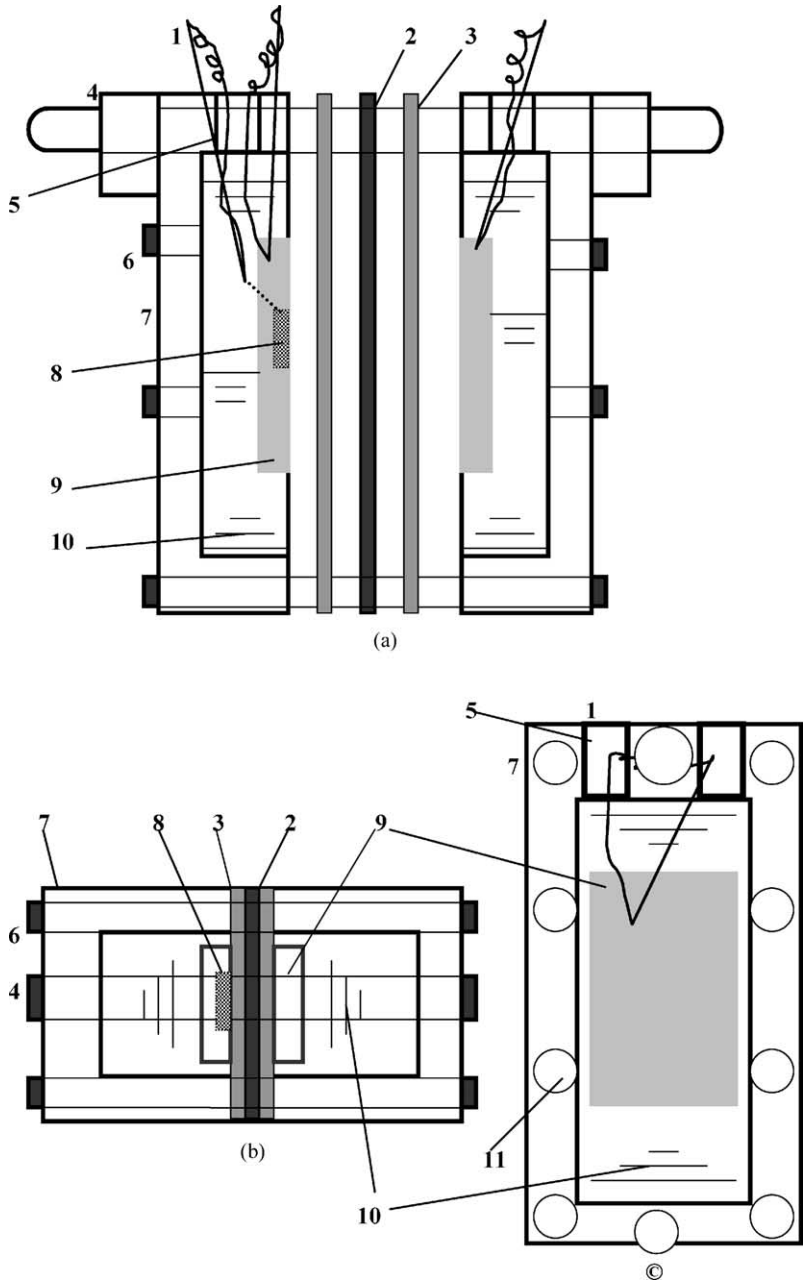

Fig. 2. Details of the rotary cell. (a) Side view of the rotary cell. (b) Cross-sectional view (top) of the rotary cell. (c) Cross-sectional view of the electrode chamber. (1) Connection wires, (2) membrane, (3) gaskets, (4) stainless steel rods, (5) holes for discharging of gas and electrolytes, (6) bolts and screws, (7) polypropylene block, (8) reference electrode, (9) working and counter electrodes, (10) electrolytes, (11) holes for the bolts and screws.

same microscope, combined with a ROUTEC UHV Dewar Detector, was used to perform EDX analysis. For preparation of the SEM samples, the catalysed titanium mesh electrodes were cut into proper pieces and were stuck onto the special disks. It was not possible to obtain absolute values of the composition of the deposits because of the mesh structure. However, the catalyst loading can be obtained during the preparation procedure and informative comparisons can be made based on the measured microscopic data.

Fig. 3 presents a scanning electron micrographs of the catalysed Ti mini-mesh prepared at controlled potential, with a loading of $2\,\text{mg Pt cm}^{-2} + 1\,\text{mg Ru cm}^{-2}$. The EDX measurement of the same mesh sample showed several characteristic peaks of Pt and Ru (not shown here), suggesting that both Pt and Ru were deposited onto the Ti mini-mesh. The SEM micrograph of the Pt–Ru/Ti mini-mesh shows that the Pt and Ru particles are distributed homogeneously across the matrix as a typical granular dense microstructure, although macropores or defects existed on the surface (Fig. 3). The electrode shows significant phase segregation and discrete regions of substrate (dark) and Pt–Ru particles (white) are observed. Small particles were deposited among the large

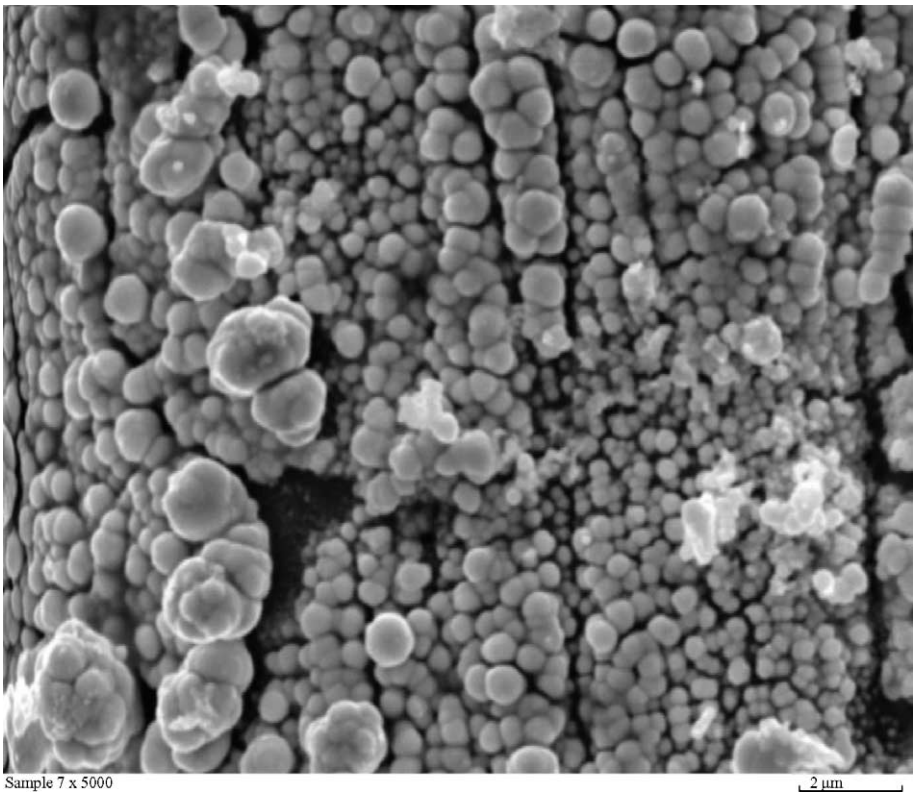

Fig. 3. Scanning electron micrograph of the Pt–Ru (2 mg Pt cm^{-2} + 1 mg Ru cm^{-2})/Ti mini-mesh (5000×) before use.

particles. The particle size changed from several nanometers to 200 nm. Some larger clusters (up to 1.5 μm in diameter), produced from aggregation of small grains, were observed. Consequently, there were a great number of boundaries or interfaces between Pt and Ru particles of different sizes, which form stack microstructure of the catalyst particles (Fig. 3) and constitute a very rough surface of the electrodeposited layer. All of these features contribute to build a high effective surface area of the electrode to promote high catalytic activity of this type of electrode. In principle, quantitative data regarding the high surface area can be obtained from CO stripping voltammetry. There are some technical problems to collect reproducible data from our mesh electrodes. Further research is needed to address the problems.

It is worthwhile to note that typically the Pt–Ru/Ti mini-mesh electrodes gave nearly the same SEM micrographs after use for the methanol oxidation, i.e. there was no observable change resulting from the use.

Conventional carbon supported electrodes were prepared for comparison. Pt–Ru catalysts used were: Pt 20 wt.%; Ru 10 wt.% on Vulcan XC-72R carbon (Electrochem. Inc., USA) or 35 wt.% Pt; 15 wt.% Ru or catalyst 40 wt.% Pt; 20 wt.% Ru on Ketjen black carbon (Johnson Matthey, UK). Each of the electrodes consisted of a backing layer, a gas diffusion layer and a reaction layer. A teflonised carbon cloth (E-TEK, type A) of 0.35 mm thickness was employed as the backing layer in both electrodes. To prepare the gas diffusion layer, the required quantity of isopropanol was added to a pre-teflonised Ketjen black carbon to make the paste required. The resulting paste was spread onto the carbon cloth and dried in an air oven at 85 °C for 5 min. To prepare the reaction layer, the required quantity of Pt–Ru/C was mixed with 10 wt.% teflonised carbon. The required quantity of Nafion solution was added to the mixture with continuously stirring. The resulting paste was spread onto the gas diffusion layer of the electrode and dried in an air oven at 85 °C for 5 min. The catalyst content on the anode was maintained at a level of 2 mg Pt cm^{-2} + 1 mg Ru cm^{-2}, the same as used for the Ti mini-mesh electrodes. Finally, a thin layer of Nafion solution was spread onto the surface of each electrode. Other details were outlined elsewhere [12].

2.3. Measurements

The polarisation behaviour of the electrochemical cell in a centrifugal field or stationary was investigated with a Model 273 EG&G Princeton Potentiostat/Galvanostat controlled by M270/250 electrochemistry software (version 4.11). Three techniques were used, i.e. linear sweep voltammetry, galvanostatic polarisation and potentiostatic polarisation. The linear sweep voltammetry was employed in most of the work for the evaluation of electrodes and the effects of centrifugal fields. To get quasi-steady-state polarisation data, a scan rate of 5 mV s^{-1} was chosen throughout this work. This was reasonable because the results obtained using 1 mV s^{-1}

were similar to those at 5 mV s^{-1}. Galvanostatic polarisation technique was chosen because it can avoid gas bubble interference and is more suitable for measurements at higher currents where evolution of large quantities of gas is unavoidable. In practice, a current was applied to the working electrode and the potential was monitored until it remained constant for a specified time (5–10 min) and then the resulting potentials were recorded. The electrode polarisation was measured at current densities of 0, 10, 50, 100, 200, 300 or 400 mA cm^{-2}. In potentiostatic polarisation measurements, constant electrode potentials were applied to the electrodes, and the current density of the electrode recorded as a function of time. The applied electrode potentials ranged from open circuit potential up to 1600 mV versus RHE, depending on electrolyte and temperature. The "electrode area" used to calculate the current density was based on that projected onto the membrane; 6 cm^2 was used in most experiments. The Nafion membrane reference electrodes were regularly calibrated against a saturated calomel reference electrode. All electrode potentials are quoted against the reversible hydrogen electrode (RHE).

All measurements were repeated with fresh solution at least twice under the same conditions to ensure reproducibility. Electrolyte solutions were prepared from Analar-grade KOH, Na_2SO_4, H_2SO_4, NaCl, NaOH, HCl [BDH] and Millipore water. HPLC-grade methanol (CH_3OH, Fisons) was used.

3. Results and discussion

3.1. Methanol oxidation in a static cell

3.1.1. Effect of anode material

The effectiveness of the anode materials for methanol oxidation was evaluated using linear sweep voltammetry (LSV). Fig. 4 shows data obtained with different anode materials, operated under stationary conditions, in 1 M CH_3OH plus 0.5 M H_2SO_4 solution at 60 °C. As shown in Fig. 4, methanol oxidation proceeded at different rates for different electrode materials.

The selection of the anode substrate had a great effect on the methanol oxidation. The introduction of an "un-optimised" Ti mini-mesh electrode led to a significant improvement in electrochemical performance over the carbon supported anodes (Fig. 4). For example, at a current density of 200 mA cm^{-2}, an anode potential of 520 mV versus RHE for the catalysed Ti mini-mesh electrode was observed. This value was much lower than obtained at the carbon supported anodes, i.e. 700 and 920 mV versus RHE for the carbon cloth anode and the carbon powder anode, respectively. The Ti mini-mesh had an open structure and lower resistance than the carbon electrodes, which benefited mass transfer of methanol and reduced electrode potential at a given current. The loss of catalysts from the carbon cloth anode, as confirmed by the SEM experiments

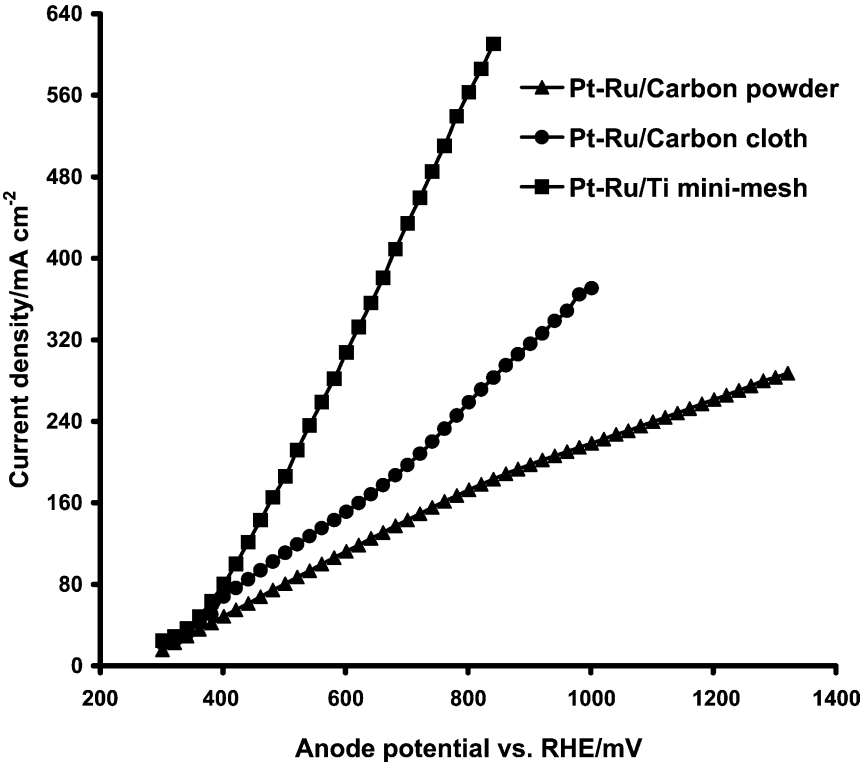

Fig. 4. Comparison between anodic polarisation curves for CH_3OH oxidation on Pt–Ru catalysed anodes with different substrates. Anode catalyst loading, 2 mg Pt cm^{-2} + 1 mg Ru cm^{-2}; cathode, Pt (2 mg Pt cm^{-2})/Ti mini-mesh; anolyte, 1 M CH_3OH + 0.5 M H_2SO_4 solution; catholyte, 0.5 M H_2SO_4 solution; scan rate, 5 mV s^{-1}; temperature, 60 °C.

(not shown here), also contributed to the poor performance of the carbon anode. The carbon powder anodes, i.e. the conventional gas diffusion electrode, showed very poor performance for methanol oxidation due to its high resistance and poor environment of mass transfer. Release of Ti ions in the electrolytes and/or damage to the membrane were not found in this work. After the operation, there was no obvious damage to the catalyst layer, which covered the Ti substrates completely. Of course, it is useful to investigate the stability of the Ti in long-term runs in further work.

Fig. 5 shows the effect of catalyst on the methanol oxidation, obtained using three catalysts in 1 M CH_3OH plus 0.5 M H_2SO_4 solution at 60 °C. The Ru/Ti mini-mesh anode showed relatively poor performance, potentials were some 150 mV greater than those observed on the Pt–Ru anode at a fixed current density. A current peak was observed at 950 mV versus RHE. This peak was not observed under the experimental potential range at the Pt–Ru electrode and shows that the Pt–Ru catalyst had higher catalytic activity than the Ru catalyst for the methanol oxidation. As anticipated, the effectiveness of the anode with the Pt coating for methanol oxidation was inferior to that of the Pt–Ru catalyst. The poisoning of Pt catalyst from surface intermediates, e.g. CO, blocked the Pt surface for further adsorption of methanol [5,9] during methanol oxidation. At Pt–Ru electrode, the surface oxides, which were able to oxidise the poisoning species during methanol oxidation, were formed at the Ru sites and thus reduced the poisoning effects [7,17,18].

The catalyst loading has a significant effect on methanol oxidation, as shown in Fig. 6. An increase of current density per milligram catalyst from 10 to 30 mA cm^{-2} mg^{-1} was observed when the catalyst loading increased from 1 mg Pt cm^{-2} + 0.5 mg Ru cm^{-2} (Pt–Ru/Ti mini-mesh B, Fig. 6) to 2 mg Pt cm^{-2} + 1 mg Ru cm^{-2} (Pt–Ru/Ti mini-mesh A, Fig. 6). A further increase in the loading had no significant benefit regarding an increase in current density [12]. Comparisons with the literature data, obtained at the Pt/carbon powder or Pt–Ru/carbon powder electrode [19,20], are made in Fig. 6. The Pt–Ru/Ti mini-mesh anodes used in this work displayed much better performance than the Pt/carbon powder anode (Pt/carbon powder, Fig. 6) for the methanol oxidation. For example, at a potential of 550 mV versus RHE, current density per milligram catalyst were 107, 84 and 50 mA cm^{-2} mg^{-1} for the Pt–Ru/Ti mini-mesh A, Pt–Ru/Ti mini-mesh B and Pt/carbon powder electrodes [19], respectively (Fig. 6). Better performance of the Pt–Ru/Ti mini-mesh A than the Pt–Ru/carbon powder [20] was also demonstrated during the methanol oxidation (Fig. 6), although the latter had higher catalyst loading, i.e. 5 mg Pt cm^{-2} + Ru cm^{-2}.

3.1.2. Effect of methanol concentration

Fig. 7 shows the effect of methanol concentration on the linear sweep voltammograms, obtained at the Pt–Ru/Ti mini-mesh anode with different methanol concentrations. Without methanol, oxygen evolution, the only observable

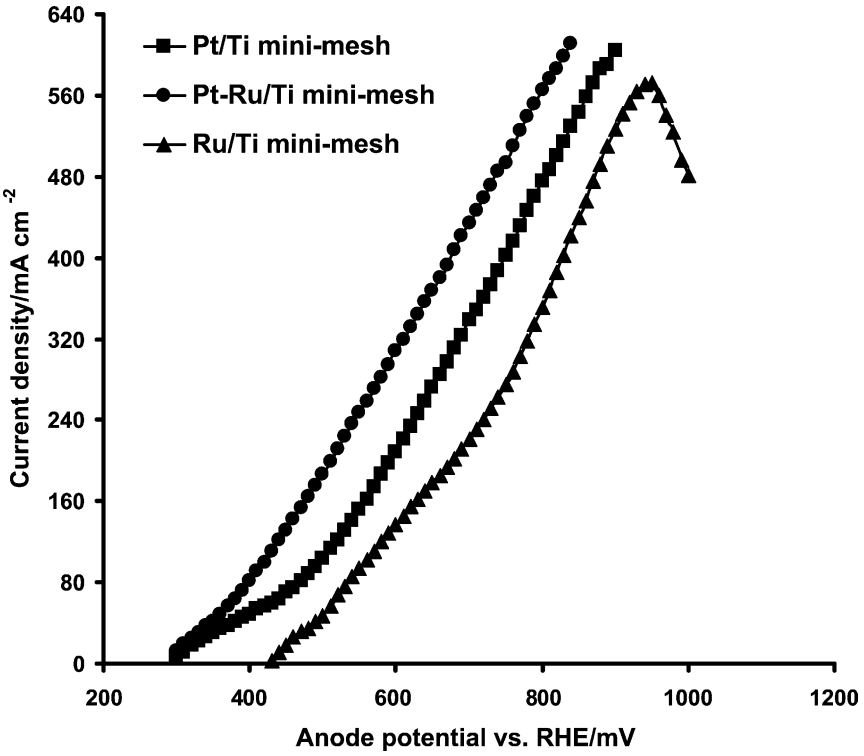

Fig. 5. Comparison between anodic polarisation curves for CH_3OH oxidation on different anodes. Anode catalyst loading, 2 mg Pt or Ru cm^{-2} for the Pt or the Ru/Ti mini-mesh anode and 2 mg Pt cm^{-2} + 1 mg Ru cm^{-2} for the Pt–Ru/Ti mini-mesh anode. Other conditions, same as those in Fig. 4.

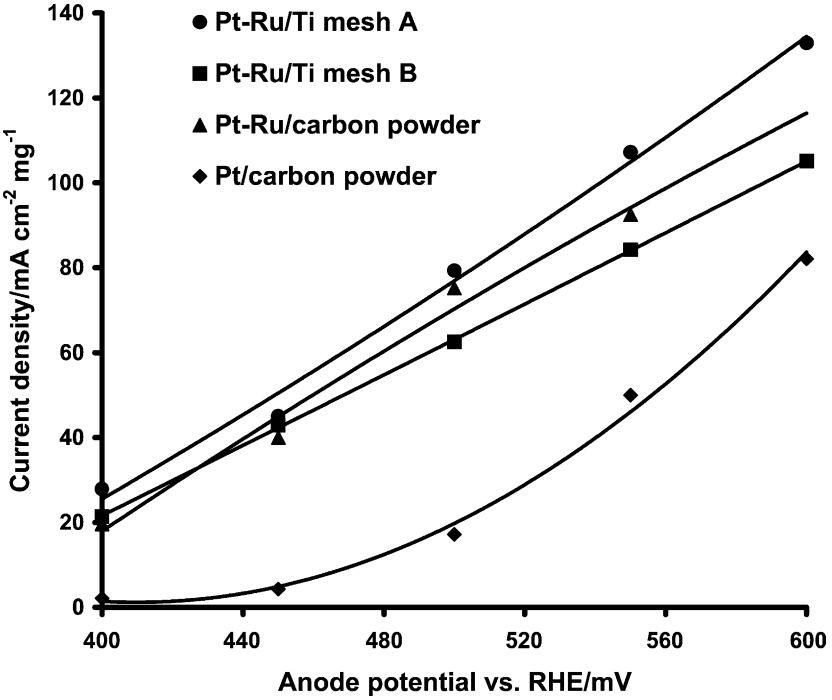

Fig. 6. Steady-state anodic polarisation curves showing the effect of catalyst loading on activity for methanol oxidation. Conditions for the Pt–Ru/Ti mini-meshes: anode catalyst loading, 2 mg Pt cm^{-2} + 1 mg Ru cm^{-2} (Pt–Ru/Ti mini-mesh A) or 1 mg Pt cm^{-2} + 0.5 mg Ru cm^{-2} (Pt–Ru/Ti mini-mesh B); anolyte, 1 M CH_3OH/0.5 M H_2SO_4 solution; cathode, Pt (2 mg Pt cm^{-2})/Ti mini-mesh; catholyte, 0.5 M H_2SO_4 solution; temperature, 60 °C; data collection method, chronoamperometry. Conditions for the Teflon-bonded Pt/carbon powder electrode (from [19]): anode catalyst loading, 3 mg Pt cm^{-2}; anolyte, 1 M CH_3OH/2.5 M H_2SO_4 solution; cathode, Au plates; catholyte, 2.5 M H_2SO_4 solution; temperature, 60 °C. Conditions for the Teflon-bonded Pt–Ru/carbon powder electrode (from [20]): anode catalyst loading, 5 mg Pt cm^{-2} + Ru cm^{-2}; anolyte, 1 M CH_3OH/0.5 M H_2SO_4 solution; temperature, 60 °C.

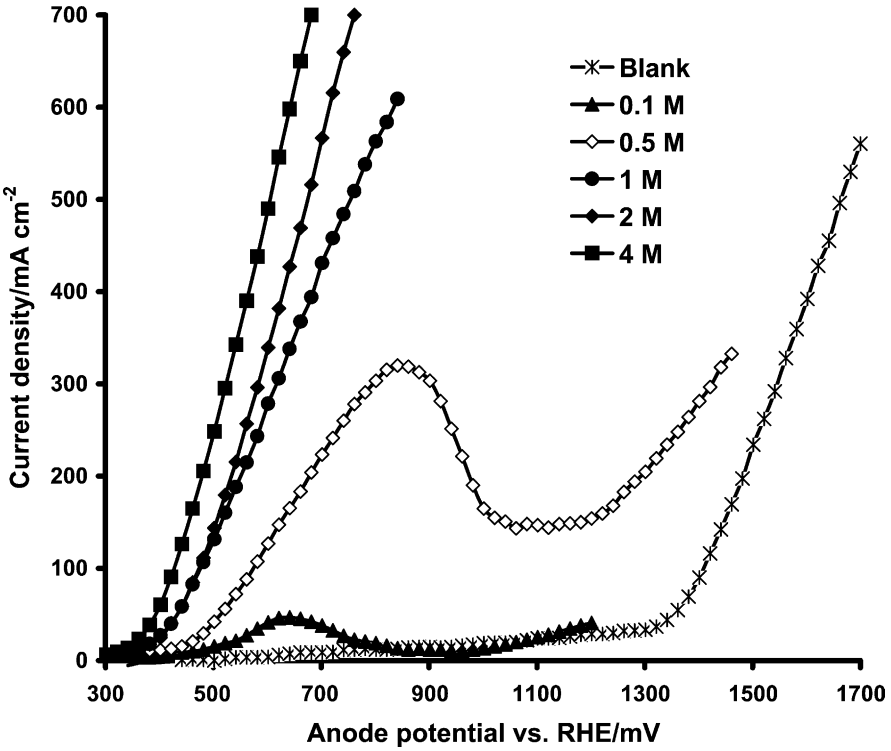

Fig. 7. Linear sweep voltammograms for methanol oxidation at a Pt–Ru/Ti mini-mesh anode in different concentrations. Methanol concentration: shown in the figure (blank: no methanol). Other conditions: same as those in Fig. 4.

reaction in 0.5 M H_2SO_4 solution, was not apparent until the potential reached 700 mV versus RHE. The current peaks were observed at 640 and 860 mV versus RHE in the presence of 0.1 and 0.5 M methanol, respectively, indicating mass transfer limitation with these solution concentrations. With methanol concentration of 1 M or above, methanol was effectively oxidised from low potentials, e.g. 300 mV versus RHE, and no oxidation peak was observed under the measured current range, suggesting that the Pt–Ru catalysts had high catalytic activity for the methanol oxidation. This was further demonstrated by decrease in potential, at a constant current density, with increasing methanol concentration. For example, at 300 mA cm^{-2}, the anode potential were 800, 620, 580 and 520 mV versus RHE for 0.5, 1, 2 and 4 M methanol solutions, respectively. The maximum anodic current density at a given anode potential was achieved in the 4 M methanol solution. However, such a high concentration should be avoided in practical fuel cells because high methanol concentration will enhance methanol crossover from anode to cathode.

The anodic current in the presence of methanol solution (Fig. 7) was mainly produced by methanol oxidation, which was confirmed by chromatography where the only detectable product was carbon dioxide and no intermediates from methanol oxidation were found. This suggested that methanol underwent complete oxidation to carbon dioxide. The intermediates, if formed, were oxidised at the anode, leaving no soluble products in the solution.

Fig. 8 shows the effect of methanol concentration on current density at three potentials, obtained from the chronopotentiometric measurements. An apparent reaction order of the methanol oxidation on the Pt–Ru/Ti mini-mesh anode, obtained from Fig. 8, was 0.8 with respect to methanol concentration. This value was in the range of those previously reported [21–23].

It is a general belief that the optimum methanol oxidation occurs in solutions with methanol concentration around 2.5 M. It was also found that the effect of methanol concentration was related to electrode properties. For example, at Pt-poly(*o*-phenylenediamine)/graphite or glass carbon electrodes, the currents of methanol oxidation levelled off from 0.7 M methanol solution. The observation was attributed to the saturation of active sites at the electrode surfaces [24]. In our case, the currents of methanol oxidation increased rapidly until 2 M and a slow increase in the oxidation currents was still observed until 4 M. One possible explanation is that there are more active sites in our electrodes, compared to the foil electrodes. Further work is required to understand the observation thoroughly.

3.1.3. *Effect of temperature*

Fig. 9 shows the effect of temperature on the methanol oxidation. An oxidation current peak appeared at 25 °C due to mass transfer limitation at this temperature. At higher temperatures, the oxidation became more facile, e.g. above 500 mV versus RHE, a doubling in current density at a fixed

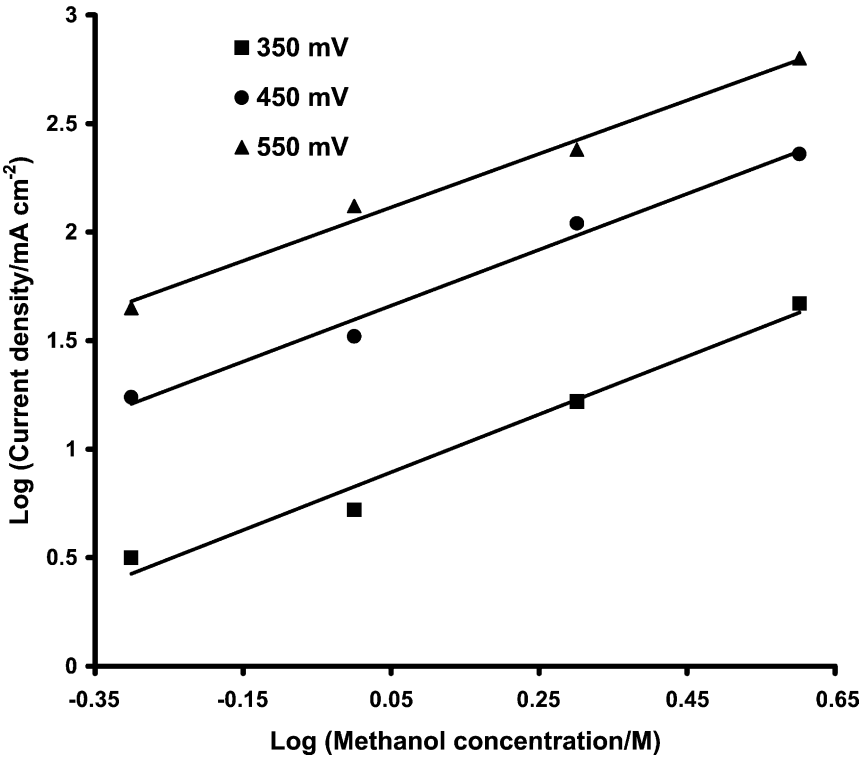

Fig. 8. Effect of methanol concentration on methanol oxidation. Data collection method, chronoampotentiometry; overpotential, shown in the figure; other conditions, same as those in Fig. 6.

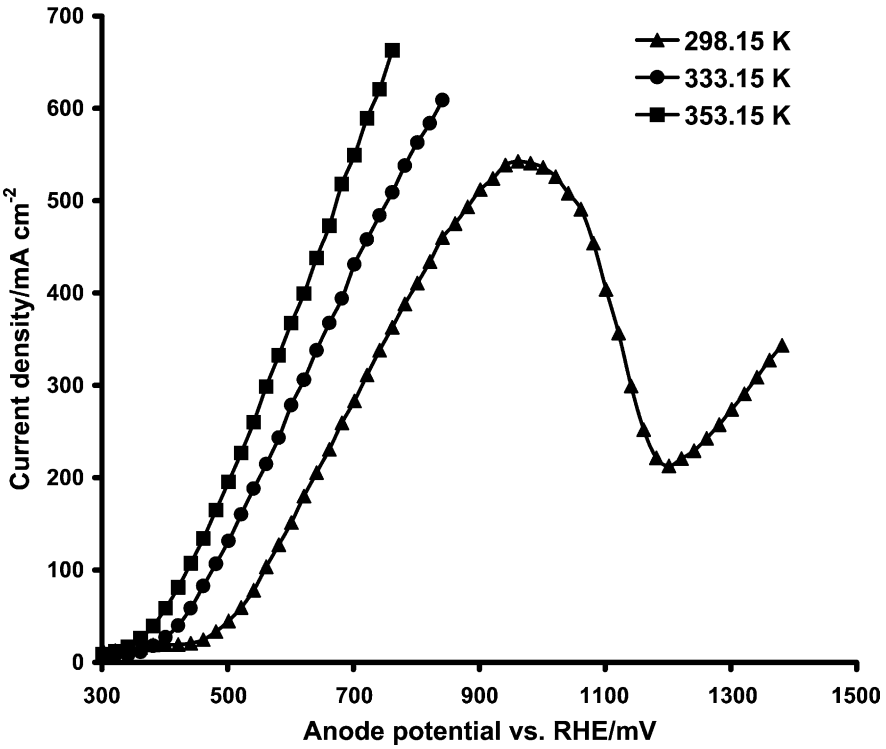

Fig. 9. Linear sweep voltammograms for methanol oxidation at a Pt–Ru/Ti mini-mesh anode in different temperatures. Temperature, shown in the figure; other conditions, same as those in Fig. 4.

potential was observed with increasing the temperature from 25 to 80 °C. These observations agreed with those reported, i.e. the effect of poisoning during methanol oxidation was less significant at higher temperatures, e.g. around 60 °C and above [20]. The exchange current density increased with increasing temperature.

3.1.4. Effect of supporting electrolyte

Fig. 10 shows the polarisation curves obtained on a Pt–Ru/Ti mini-mesh electrode, with different supporting electrolytes, for oxidation of 1 M CH_3OH solution at 60 °C. As can be seen, methanol oxidation occurred in different potential regimes in alkaline, neutral, and acidic media. For example, the oxidation potentials were 510 and 630 mV versus RHE at 300 mA cm^{-2} in the alkaline, acidic and neutral media, respectively. A greater rate of increase in current density with potential was observed in the acidic medium, at higher potentials above 600 mV versus RHE, compared with the neutral solution.

The effect of concentration of supporting electrolyte on methanol oxidation was investigated in sulphuric acid solutions and the typical results were shown in Fig. 10. The rate of the methanol oxidation increased significantly with increasing the acid concentration. For example, at a potential of 700 mV versus RHE, the current density increased from 190 to 450 mA cm^{-2} when the acid concentration increased from 0.1 to 1 M. A further increase of the acid concentration led to small increase in current density. Higher acid concentration contributed to reduce the ohmic resistance of the electrolytes and resulted in higher current densities at a given potential.

3.2. Methanol oxidation in a centrifugal field

The main functions of a centrifugal field are promoting mass transport and disengaging gas bubbles from the electrode surfaces, the electrolyte and the membrane. These functions should benefit a conventional DMFC through improved mass transfer and removal of CO_2 gas from electrodes, electrolytes and membrane. Fig. 11 shows the effect of relative acceleration rate on anodic polarisation curves for methanol oxidation in the rotary electrochemical cell. When the cell was operated statically, methanol was effectively oxidised at the Pt–Ru/Ti mini-mesh anode in the observed potential range, with a rapid increase of current density after 300 mV versus RHE, due to the high catalytic activity of Pt–Ru catalysts for methanol oxidation. As expected, electrochemical behaviour of methanol oxidation was greatly affected by the applied centrifugal force, with a significant enhancement in performance as the relative acceleration rate was increased. The most significant effect was observed after 400 mV versus RHE where current density increased up to 700 mA cm^{-2} at 700 mV versus RHE at an acceleration rate of 190, for example.

The effect of centrifugal field on the anode potential is clearly seen in Fig. 12 where the reduction in anode potential with a relative acceleration rate is plotted at different current densities. The reduction in anode potential

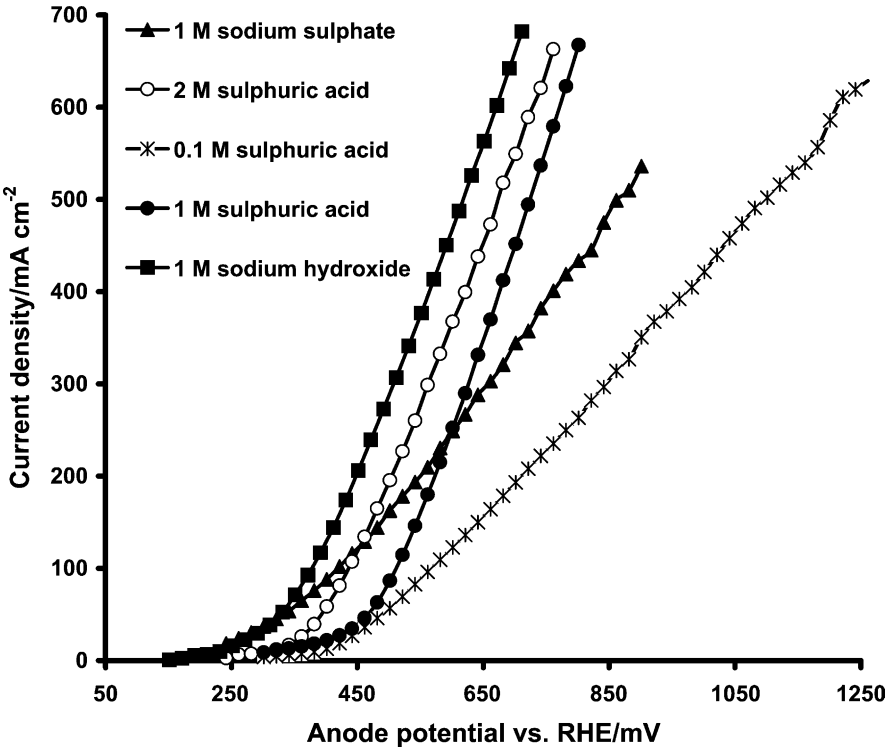

Fig. 10. Linear sweep voltammograms for oxidation of 1 M methanol in different supporting electrolytes. Supporting electrolyte, shown in the figure; other conditions, same as those in Fig. 4.

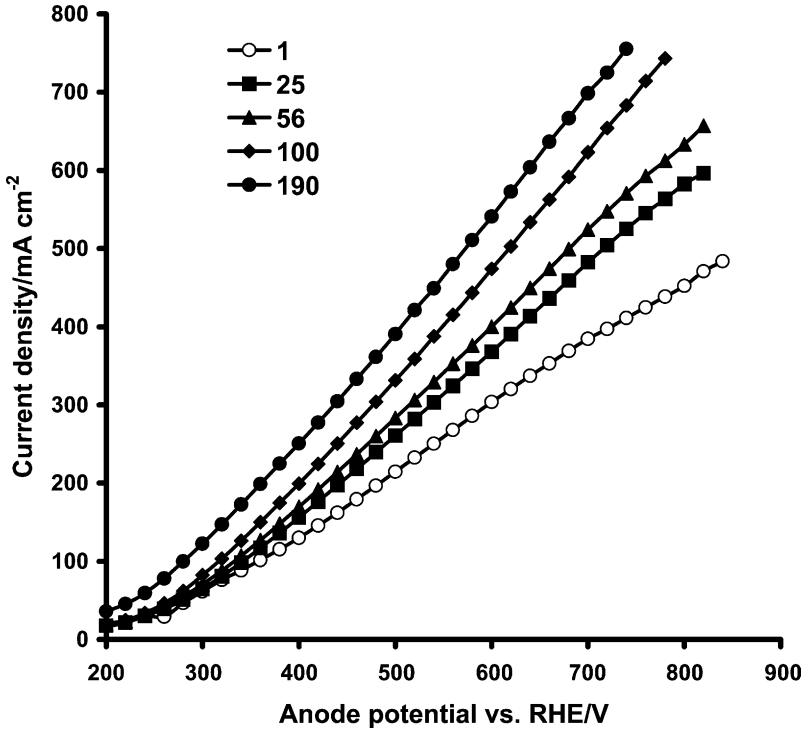

Fig. 11. Anodic polarisation curves for CH_3OH oxidation in the rotary electrochemical cell. Anode, Pt–Ru/Ti mini-mesh (2 mg Pt cm^{-2} + 1 mg Ru cm^{-2}); cathode, Pt (2 mg Pt cm^{-2})/Ti mini-mesh; anolyte, 1 M CH_3OH + 0.5 M H_2SO_4 solution; catholyte, 0.5 M H_2SO_4 solution; scan rate, 5 mV s^{-1}; temperature, 80 °C.

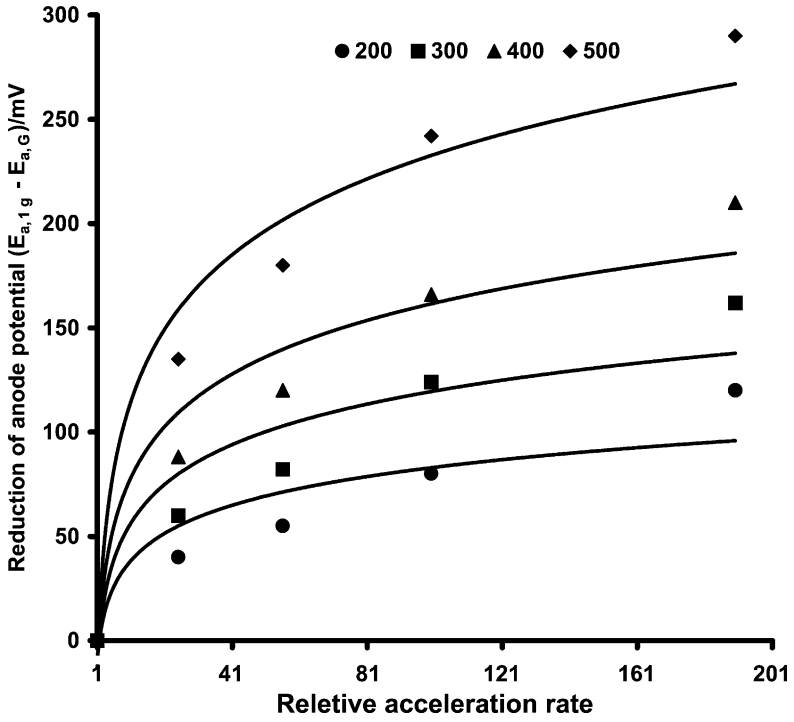

Fig. 12. Reduction of anode potential against relative acceleration rate plots for CH_3OH oxidation in the rotary cell. Current density, shown in the figure (mA cm^{-2}); other conditions, same as those in Fig. 11.

increased with increasing relative acceleration rate. The effect was more significant at higher current densities than at low current densities, as shown in Fig. 12. For example, the maximum potential reduction was 120 mV at 200 mA cm^{-2}, which increased to 290 mV at 500 mA cm^{-2}. It is easy to understand this performance enhancement by comparing different operating conditions of the rotary cell and the static cell. In the static cell, mass transfer limitation of methanol

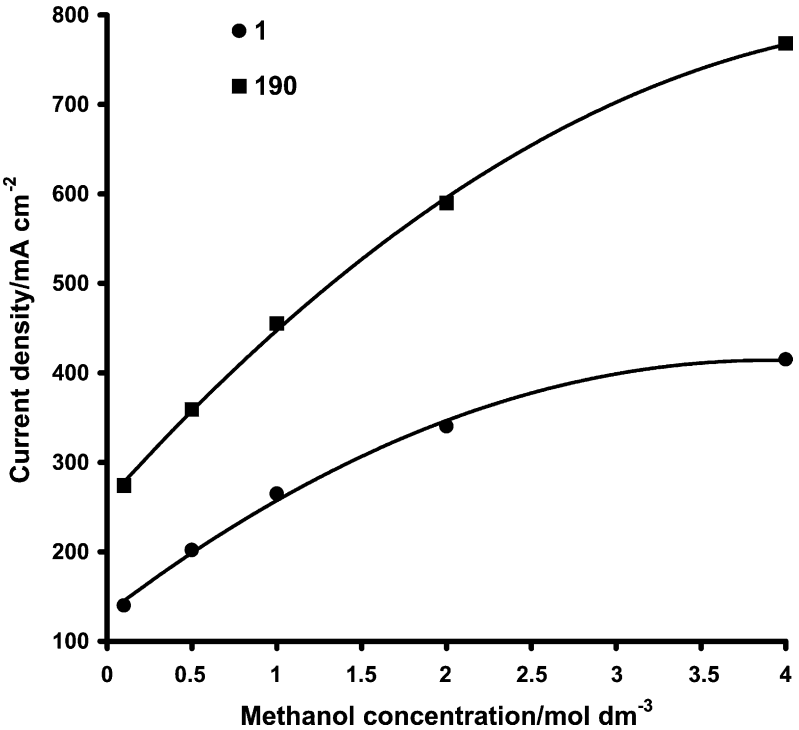

Fig. 13. Enhancement of the concentration effect for CH_3OH oxidation in a centrifugal field—current density (at 500 mV vs. RHE) vs. methanol concentration curves. Conditions: same as those in Fig. 11.

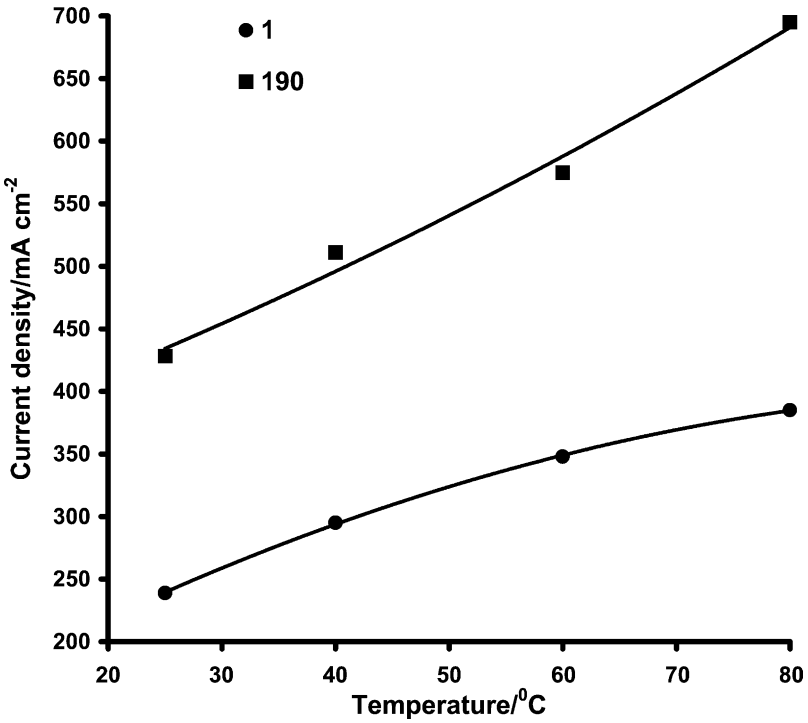

Fig. 14. Enhancement of the temperature effect for CH_3OH oxidation in a centrifugal field—current density (at 700 mV vs. RHE) vs. temperature curves; temperature range, 25–80 °C; other conditions, same as those in Fig. 11.

would be very crucial at high current densities where more gas bubbles would be evolved and thus increase the resistance, compared with that at low current densities. Application of a centrifugal field to the cell greatly enhanced the mass transfer within the cell and efficiently disengaged the bubbles from the electrode surfaces, the electrolyte and the membrane and, consequently, the methanol oxidation process was improved, as shown in Fig. 12.

The effect of methanol concentration on the methanol oxidation in the centrifugal field is shown in Fig. 13, obtained from the controlled potential measurements. The current density at an acceleration rate of 190 was always greater than that in the gravitational field for a given concentration. A higher rate of increase in the current density with increasing the concentration was observed at an acceleration rate of 190, compared with that in the gravitational field. For example, at an acceleration rate of 190, the average rate increase was about 120 mA cm^{-2} M^{-1} from 0.1 to 4 M, cf. in the gravitational field, i.e. about 68 mA cm^{-2} M^{-1}.

The effect of temperature on current density at a potential for methanol oxidation in a centrifugal field is shown in Fig. 14. The current density increased, in both the gravitational field and the centrifugal field, with increasing temperature at a given anode potential. However, the average rate of increase of the current density was higher at an acceleration rate of 190 than in the gravitational field, i.e. 4.86 and 2.66 mA cm^{-2} $°C^{-1}$, respectively. This means that high temperature further improved the methanol oxidation in the centrifugal field.

4. Conclusions

High efficiency of Pt–Ru/Ti mini-mesh anode for methanol oxidation was demonstrated and the potential reductions up to 380 mV was achieved at a current density of 200 mA cm^{-2}, compared with the carbon supported Pt–Ru anodes. The catalysed Ti mini-mesh electrode was capable of providing micropores for gas access, micropores for liquid access and conductive paths for electron access. The problems in conventional carbon supported electrodes, such as high ohmic losses and low ionic conductivities, have been overcome to a large extent using the catalysed Ti mini-mesh.

Methanol oxidation was improved in a centrifugal field, where further reductions of anode potential up to 150 mV, at 200 mA cm^{-2} and 90 °C, were realised at an acceleration rate of 190, compared with that achieved in the gravitational field. The performance improvement was attributed to the centrifugal fields, promoting mass transfer and enhancing gas bubble disengagement from the electrode surfaces, the electrolyte and the membrane.

A significant effect of methanol concentration on the methanol oxidation was observed, particularly in solutions with methanol concentration below 2 M. Similarly, increasing temperature greatly improved methanol oxidation. An increase in concentration of the supporting electrolyte also led to an improvement of the anode performance. The improvements in performance, on increasing the concentration and the temperature, were more pronounced in a centrifugal field than in the gravitational field.

References

[1] B.D. McNicol, D.A.J. Rand, K.R. Williams, J. Power Sources 100 (2001) 47.
[2] S. Wasmusa, A. Kuverbc, J. Electroanal. Chem. 461 (1999) 14.
[3] K. Scott, W. Taama, J. Cruickshank, J. Appl. Electrochem. 70 (1998) 40.
[4] A.K. Shukla, P.A. Christensen, A. Hamnett, M.P. Hogarth, J. Power Sources 55 (1995) 87.
[5] P.A. Christensen, A. Hamnett, J. Munk, G.L. Troughton, J. Electroanal. Chem. 370 (1994) 251.
[6] B.B. Cattaneo, S. Wasmus, B.L. Mishima, W. Vielstich, J. Appl. Electrochem. 23 (1993) 625.
[7] J.B. Goodenough, A. Hamnett, B.J. Kennedy, R. Manoharan, S.A. Weeks, J. Electroanal. Chem. 240 (1988) 133.
[8] J. O'M. Bockris, B.E. Conway, E. Yeager, R.R. White (Eds.), Comprehensive Treatise of Electrochemistry, vol. 3, Plenum Press, New York, 1981.
[9] P.A. Christensen, A. Hamnett, Techniques and Mechanisms in Electrochemistry, Blackie, London, 1994.
[10] H. Cheng, K. Scott, C. Ramshaw, Chlorine evolution in a centrifugal field, J. Appl. Electrochem. 32 (2002) 831.
[11] H. Cheng, K. Scott, C. Ramshaw, Intensification of water electrolysis in a centrifugal field, J. Electrochem. Soc. 149 (2002) D172.
[12] H. Cheng, Ph.D. Thesis, University of Newcastle upon Tyne, Newcastle upon Tyne, 1999.
[13] G. Meli, J.-M. Leger, C. Lamy, R. Durand, J. Appl. Electrochem. 23 (1993) 197.
[14] E.J. Taylor, E.B. Anderson, N.R.K. Vilambi, J. Electrochem. Soc. 139 (1992) L45–L46.
[15] M. Shen, Y. Chen, in: N.M. Prout, J.S. Moorhouse (Eds.), Modern Chlor-Alkali Technology, vol. 4, Elsevier, London, 1990, p. 149.
[16] D.W. DeWulf, A.J. Bard, J. Electrochem. Soc. 135 (1988) 1977.
[17] S. Trasatti, W.E. O'Grady, in: H. Gerischer, C.W. Tobias (Eds.), Advances in Electrochemistry and Electrochemical Engineering, vol. 12, Wiley, New York, 1981, p. 177.
[18] B. Beden, J.M. Leger, C. Lamy, in: J'O.M. Bockris, B.E. Conway, R.E. White (Eds.), Modern Aspects of Electrochemistry, vol. 22, Plenum Press, New York, 1992, p. 97.
[19] J.B. Goodenough, A. Hamnett, B.J. Kennedy, R. Manoharan, S.A. Weeks, Electrochim. Acta 35 (1990) 199.
[20] S. Surampudi, S.R. Narayanan, E. Vamos, H. Frank, G. Halpert, A. LaConti, J. Kosek, G.K.S. Prakash, G.A. Olah, J. Power Sources 47 (1994) 377.
[21] H.A. Gasteiger, N. Markovic, P.N. Ross, E.J. Cairns, J. Electrochem. Soc. 141 (1994) 1795.
[22] A.V. Tripkovic, K.D. Popovic, J.D. Momcilovic, D.M. Drazic, Elechtrochim. Acta 44 (1998) 1135.
[23] N.A. Mayorova, O.A. Khazova, V.S. Bagotzky, J. Solid State Electrochem. 2 (1998) 262.
[24] S.M. Golabi, A. Nozad, J. Electroanal. Chem. 521 (2002) 161–167.